Microstructure, Mechanical Properties, and Fracture Behavior of Liquid Rubber Toughened Thermosets

YI-BING ZENG,* LIAN-ZHENG ZHANG, WEI-ZHOU PENG, and QIAO YU

Beijing Research Institute of Materials & Technology, P.O. Box 9211-73-17, Beijing 100076, People's Republic of China

SYNOPSIS

Phenolic epoxy resin was toughened by carboxyl-randomized butadiene acrylonitrile copolymer (CRBN) for use as composite matrix. By adding different parts of butadiene acrylonitrile copolymer (BN-26, without carboxyl contained) to CRBN, different sizes of rubber domains and different numbers of chemical bondings between the resin matrix and the rubber phase were obtained. It is found that small rubber particles (less than 0.1 μm) are cavitated during the crack development. The interaction between secondary crack zones caused by the cavitation makes the fracture toughness K_{IC} of the materials high; by comparison, a local stress-whitened zone is produced in the material with large rubber particles (more than 0.1 μm) when it is subjected to tensile stress. In this case, the flexure strength σ_f of the material is great. Using ultrasection and TEM techniques, the stress-whitened zone was shown to be caused by the special multiple-phase structure of the material, in which many caves and "macrocrazes" coexist.

INTRODUCTION

To improve the toughness of a glass thermoset resin, such as epoxy resin, the most useful and practical method is toughening by adding a small amount of liquid rubber to form discrete particles in the resin matrix. The research work has been carried out for over 30 years.[1] The dispersed rubber phase, which separates from the resin before gelation,[2] plays an important role in the toughness improvement of the material.

However, it is not very clear so far what effect the size of the rubber phase has on toughness improvement in epoxy resin systems. Sultan and McGarry[3] showed the effect of the rubber particle size on deformation mechanisms in the epoxy system: shear mechanism is enhanced by the presence of small rubber particles (a few hundred Å in diameter), whereas crazing appears as the main reason for the toughness improvement of the material with large rubber particles (1.5–5 μm), and the fracture energy of such material is five times as much as that with small rubber particles. Many researchers believed that optimal toughening was obtained under conditions of combined shear and craze deformations, which are obtainable when both large and small rubber particles present in bimodal distribution.[4–6] However, A.F. Yee concluded in NASA CR 3718 Report that the rubber phase size is not important for the toughening result.

In this work, we show how morphology of carboxyl-randomized butadiene acrylonitrile copolymer (CRBN) toughened phenolic epoxy resin relates to the mechanical properties and fracture behavior of these systems.

EXPERIMENTAL

Materials

Phenolic epoxy resin with average molecular weight of 551 (F-51) was used. The liquid rubbers were CRBN and butadiene acrylonitrile copolymer (BN-26, without carboxyl contained) with average molecular weights of 1862 and 1181, respectively. The isomers of methyltetrahydrophtalic anhydride (HK-

* To whom correspondence should be addressed.

Journal of Applied Polymer Science, Vol. 42, 1905–1910 (1991)
 CCC 0021-8995/91/071905-06$04.00

021) was used as curing agent, and 2-ethyl-4-methylimidazol (2,4-EMI) was used as curing accelerator. The molecular formulae of the materials used here are listed as following:

F-51:

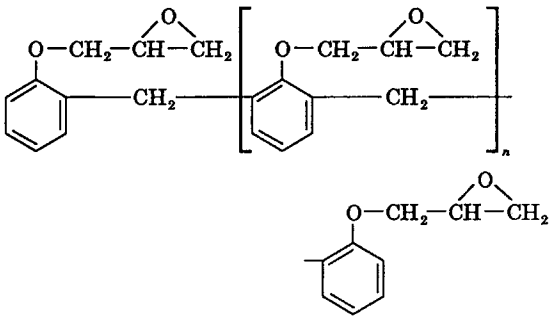

CRBN:

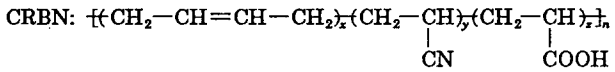

BN-26:

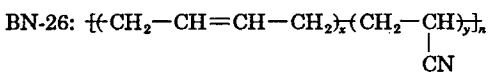

HK-021:

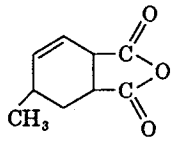

2,4-EMI:

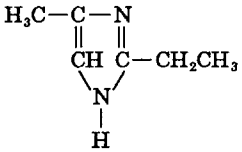

Specimen Preparation

Resin, liquid rubbers, curing agent, and curing accelerator were mixed at room temperature according to the formulations listed in Table I, and then degassed in a vacuum oven at 60°C. The mixture was next poured into a mold and cured under the condition of 80°C/2 h + 120°C/2 h.

Three-point bending specimens (Fig. 1) were cut from the cast epoxy plaques. In Figure 2, single edge notched specimens were used to determine the fracture toughness K_{IC} of the materials. Each specimen was notched using a saw. A crack that appears sharp was produced by a few taps with a hammer on a fresh razor blade inserted into the cut notch.

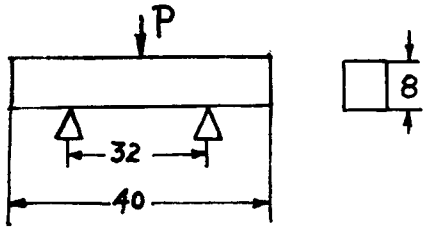

Figure 1 The specimen for flexure strength σ_f.

Morphology Observation

Transmission electron microscope (TEM), Model H-700, Hitachi Corporation, was used. Samples of the materials were stained in a 1% solution of osmium tetraoxide (OsO_4/THF),[7] and then microtomed by a diamond blade into sections with thickness about 400–500 Å to be suitable for observation.

Scanning electron micrographs (SEM) were obtained on fracture surfaces after a three-point bending test. The fractured surfaces were sputtered with gold before observation.

Mechanical Testing

The three-point bending test was conducted on an Instron Model 1195 mechanical tester. The test speed was 1 mm/min. The flexure strength σ_f and fracture toughness K_{IC} were given by:[8]

$$\sigma_f = 3P_c l/2bh, \qquad \text{MPa}$$

$$K_{IC} = P_c y\left(\frac{a}{h}\right)\Big/ bh^{1/2}, \qquad \text{Nm}^{-3/2},$$

where Pc = applied force at fracture, l = span, b = width, h = height, a = crack deepness, l = 4 h, b = 1/2 h.

Table I Composition and Notation

	A	B	B-1	B-2	B-3	B-4
F-51, parts	100	100	100	100	100	100
CRBN, parts	0	30	27	21	9	0
BN-26, parts	0	0	3	9	21	30
Volume fraction of rubber added	0	0.19	0.19	0.19	0.19	0.19

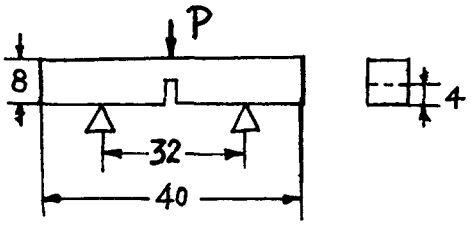

Figure 2 The specimen for fracture toughness K_{IC}.

$$y\left(\frac{a}{h}\right) = \left[7.51 + 3.00\left(\frac{a}{h} - 0.50\right)\right] \times \sec\left(\frac{a}{2h}\right) \cdot \left[t_g\left(\frac{a}{2h}\right)\right]^{1/2}.$$

RESULTS AND DISCUSSION

Morphology

The cast plaques of A and B were optically clear, while plaques of B-1, B-2, B-3, and B-4, which all contain the same amount of rubber with B, were apparently turbid. B-4 was loose and almost without any strength. Samples of B, B-1, B-2, and B-3 were stained by OsO_4 and ultrafinely sectioned, the TEMs of which are shown in Figures 3, 4, 5, and 6, respectively.

In Figure 3, the size of rubber domains is very small (40–300 Å), and the shape is irregular. The dispersed rubber domains grow evidently by adding a small amount of BN-26, which can be seen in Figure 4. With the increase of the ratio of BN-26/CRBN, the size and volume fraction of rubber particles increase, and the amount of resin that penetrates into rubber phases decreases. The shape and interface of rubber particles become more and more regular (Figs. 5 and 6). Therefore, the presence of BN-26 can promote the phase separation of CRBN in the resin.

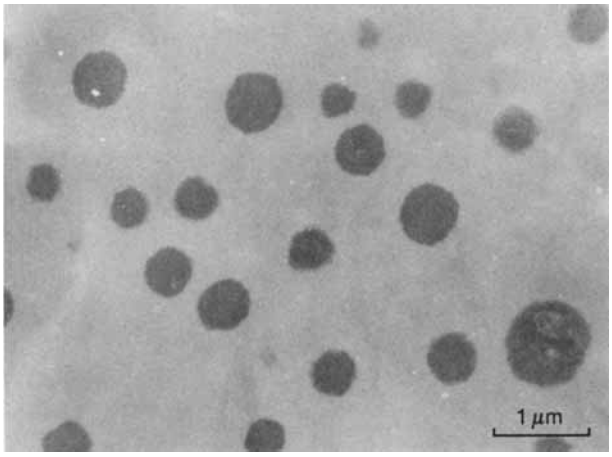

Figure 4 Transmission electron micrograph of B-1.

Mechanical Properties

The flexure strength σ_f and fracture toughness K_{IC} of these materials listed in Table II, were determined by three-point bending test. The flexure strength σ_f of B-1 with large rubber particles is greater than that of B with small ones. With the increase of the proportion of BN-26 in rubber phases, the chemical bondings between the resin matrix and the rubber phase reduce, and the σ_f values of such materials decrease. For specimens that were notched sharply,

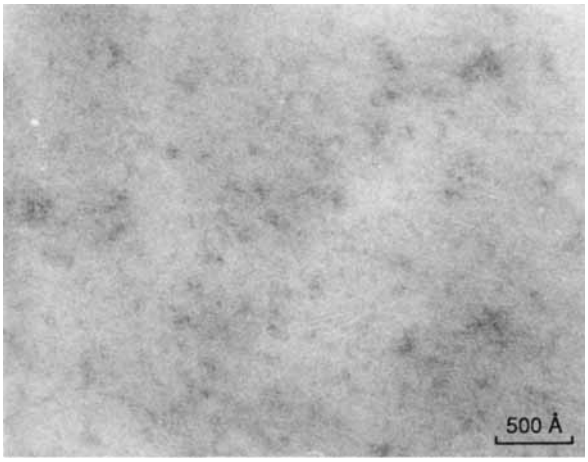

Figure 3 Transmission electron micrograph of B.

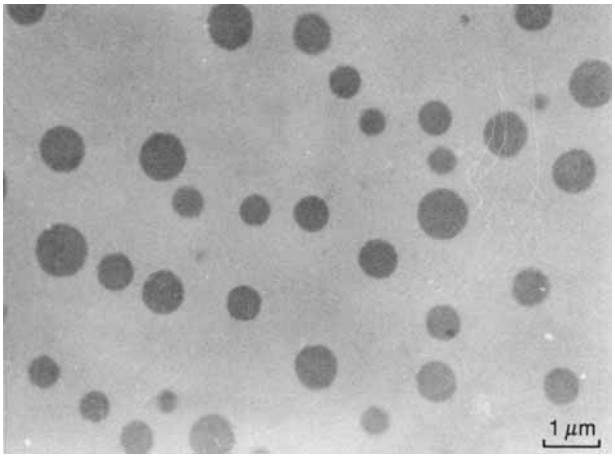

Figure 5 Transmission electron micrograph of B-2.

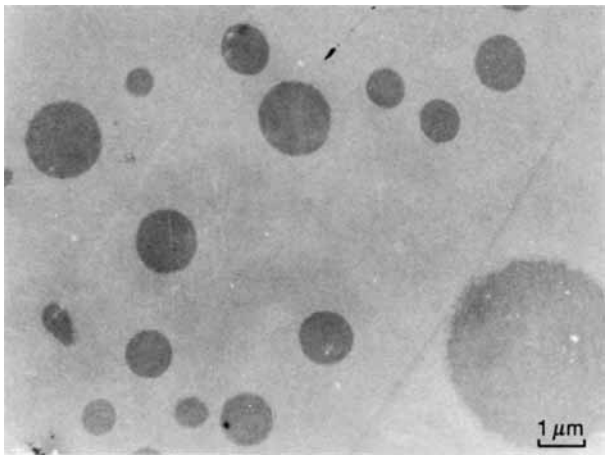

Figure 6 Transmission electron micrograph of B-3.

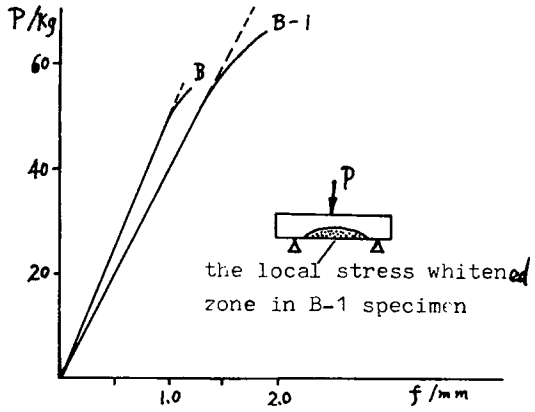

Figure 7 Load-deflection curves of B and B-1.

the fracture toughness K_{IC} of B-1 is less than that of B, indicating that the ability for large rubber particles to resist the fast development of sharp cracks in the resin matrix is not as great as that for small particles. It is noted that the yield behavior of B-1 before fracture is quite different from that of B, and a local stress-whitened zone is presented in the part subjected to the tensile stress field (see Fig. 7).

Fracture Surface Analysis

The SEM of the fracture surface of B that contains small rubber domains is shown in Figure 8. During the crack development, rubber particles are cavitated and result in a large amount of secondary crack zones. The interaction of these secondary crack zones on each resists the smooth development of crack and makes the fracture toughness K_{IC} of B high. There are many microvoids on the fracture surface of B-1 (Fig. 9), and the size of these holes is homogeneous (about 0.4 μm). Careful examination of Figure 9 reveals that the diameter of these holes is larger than the particle size in TEM graph of Figure 4 (0.3 μm). It can be deduced that the crack trajectory is along the equatorial planes of rubber particles.[9] However, the holes in the fast crack propagation zone of Figure 10 are varied in size, with an average diameter of 0.3 μm, approximately the same as the particle size in the TEM graph of Figure 4. In this case, the crack crosses discrete rubber particles directly in one plane. This is why the fracture toughness K_{IC} of B-1 is lower than that of B.

Microstructure of the Stress-Whitened Zone

The microstructure of the stress whitened zone, presented in Figure 11 and 12, is observed by TEM from OsO_4 stained sections of the stress-whitened material in Figure 7. As shown in Figure 11, there are parallel of orientated polymer materials at the crack tip, and many microcracks exist between the orientated materials. This structure is similar to that of crazes in thermoplastic polymer materials proposed by Manson and Sperling.[10] The width of the craze here is about 10 μm. The structure can be called a "macrocraze." Under most circumstances, microcracks in the craze are initiated and terminated at rubber particles. Some structures similar to caves are also found in the stress-whitened zone (Fig. 12). The cause of the formation of the stress-whitened zone is related to the particular multiple-phase microstructure in the material. When the resin matrix with large rubber particles (about 0.3 μm) is subjected to the tensile stress, the stress concentration on the interface between the resin matrix and the

Table II Mechanical Testing Results

	A	B	B-1	B-2	B-3
Flexure strength, MPa	79.8	91.6	125.7	88.6	62.0
Fracture toughness, $Nm^{-3/2} \times 10^{-5}$	8.7	11.5	9.9	9.2	8.9

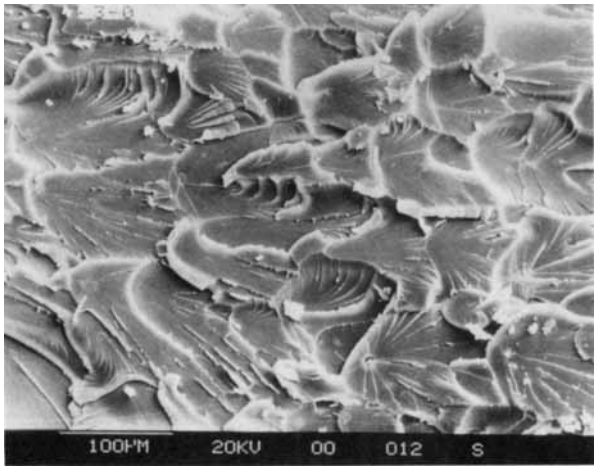

Figure 8 SEM micrograph of B specimen cleavage fractured surface.

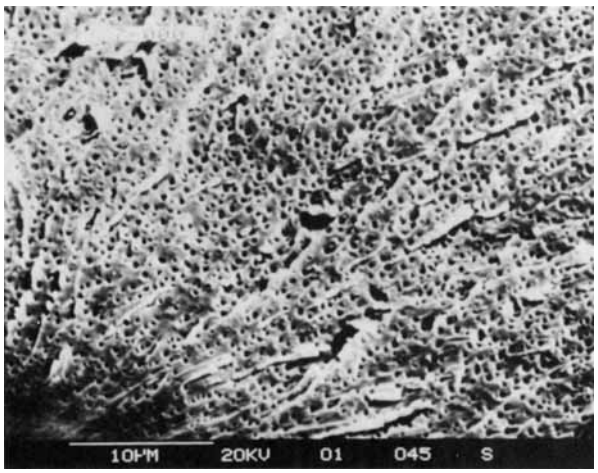

Figure 9 SEM micrograph of B-1 specimen cleavage fractured surface. Slow crack propagation.

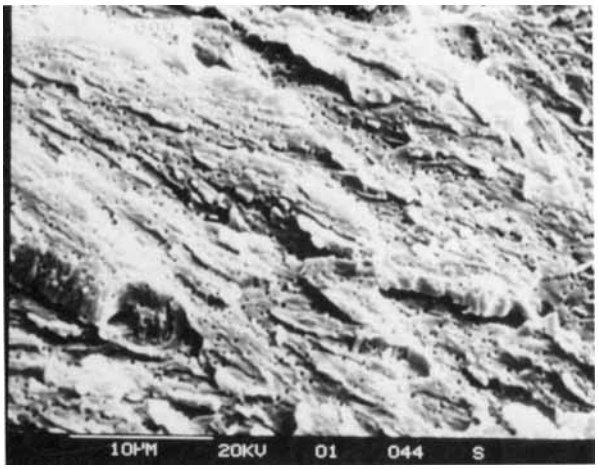

Figure 10 SEM micrograph of B-1 specimen cleavage fractured surface. Fast crack propagation.

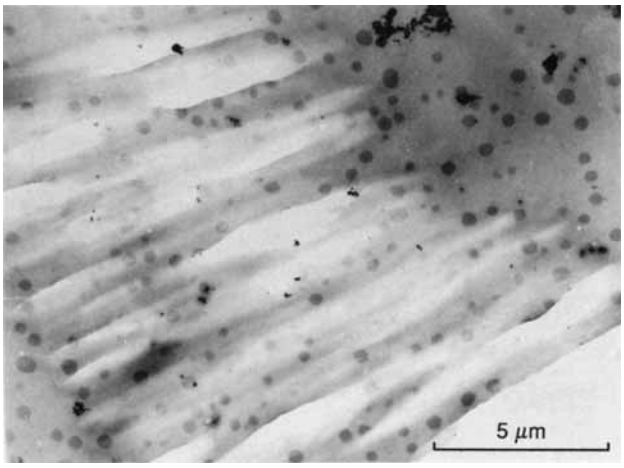

Figure 11 TEM of the local stress whitened zone in B-1 specimen.

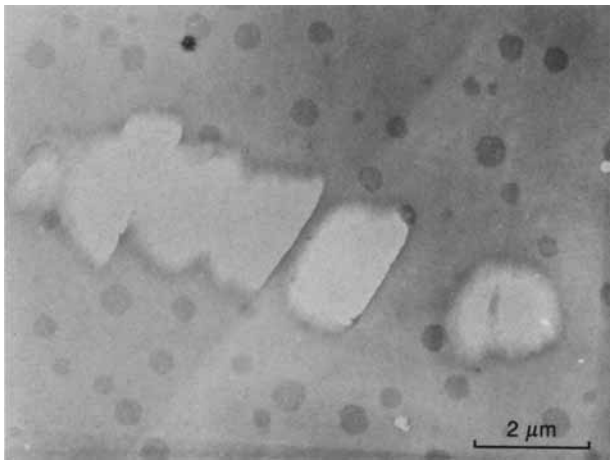

Figure 12 A cave structure in the stress-whitened zone.

rubber particle makes the particle be teared away, and then the crack develops. During the crack propagation, much energy is dissipated by crossing and bypassing rubber particles in the resin matrix. The crack is stopped when it is unable to pass the rubber phase. In this way, many microcracks are fixed and exist in the matrix to make the material whitened.

CONCLUSIONS

Three conclusions can be drawn from this study:

1. The phase separation of CRBN from phenolic epoxy resin can be promoted by adding a small amount of BN-26.

2. The flexure strength σ_f of the material with large rubber particles (about 0.3 μm) is greater than that of the material with small ones (30–400 Å). But the fracture toughness K_{IC} of the latter is higher than that of the former.
3. TEM analysis shows that many caves and macrocrazes coexist in the stress-whitened material and the phenomenon is presumed to be caused by the special multiple-phase microstructure within the material.

REFERENCES

1. A. R. Siebert, Rubber-modified thermoset resins, *Adv. Chem. Series* **208,** P179, ACS, Washington, D.C. (1984).
2. L. T. Manzione and J. K. Gillham, *J. Appl. Polym. Sci.* **26,** 889 (1981).
3. J. N. Sultan and R. C. McGarry, *Polym. Eng. Sci.* **13,** 29 (1973).
4. C. K. Riew, E. H. Rowe, and A. R. Siebert, *Adv. Chem. Series* **154,** P326, ACS, Washington, D.C. (1976).
5. W. D. Bascom, R. Y. Ting, et al., *J. Mater. Sci.* **16,** 2657 (1981).
6. Sun Yishi et al., *Polym. Commun.* (Chinese Ed.) **3,** 196 (1983).
7. C. K. Riew and R. W. Smith, *J. Polym. Sci. A-1* **9,** 2739 (1971).
8. Chu Wuyang et al., *Determination of Fracture Toughness,* Science Publishing House, Beijing, 1979.
9. E. Butta, G. Levita, et al., *Polym. Eng. Sci.* **26,** 63 (1986).
10. J. A. Manson and L. H. Sperling, *Polymer Blends and Composites,* Plenum, New York, 1976.

Received March 8, 1990
Accepted July 9, 1990